



CHORUS

This is the accepted manuscript made available via CHORUS. The article has been published as:

Akhiezer mechanism limits coherent heat conduction in phononic crystals

Yuxuan Liao, Takuma Shiga, Makoto Kashiwagi, and Junichiro Shiomi

Phys. Rev. B **98**, 134307 — Published 16 October 2018

DOI: [10.1103/PhysRevB.98.134307](https://doi.org/10.1103/PhysRevB.98.134307)

29 question that why the thermal conductivity of PnCs can be explained by only
30 considering scattering of incoherent phonons at these temperatures.

31

32 I . INTRODUCTION

33 Phononic crystals (PnCs) with specifically designed periodic structures are meant to
34 manipulate propagation of phonons using coherent effect (that is phase is preserved).
35 In such a case, phonons follow the dispersion relation of PnCs, whose branches are
36 folded with band gaps, which reduces group velocity, and hence results in reduction of
37 thermal conductivity [1]. Benefit of manipulating thermal conductivity of PnCs using
38 coherent effect is that it has smaller influence on electrons. Therefore, they are regarded
39 as attractive candidate for enhancing figure of merit of thermoelectric materials.

40 The promising prospect of controlling phonons by using the coherent effect in
41 periodic structures has triggered many experimental measurements of the thermal
42 conductivity for PnCs. Most popular class of PnCs is silicon thin films with periodic
43 holes as they can be fabricated by conventional microfabrication technique. However,
44 their thermal conductivity of PnC can be attributed to phonon coherent effect only for
45 temperatures below 10 K [2,3], and recent theoretical works have confirmed that
46 thermal conductivity of PnC seen at room temperature in some of the early works can
47 be explained by only considering scattering of incoherent phonons (i.e. phonons lose
48 phase and follow the dispersion relation of bulk crystals instead of the dispersion
49 relation of PnCs), that is to say that coherent phonons have negligible contributions to
50 the thermal conductivity of PnCs at room temperature [4,5].

51 A possible theoretical explanation for the negligible contribution of coherent
52 phonons is that the coherent transport requires atomically smooth boundary surfaces,
53 and absence of impurities and defects [6-9], which can only be realized in limited
54 structures such as superlattices [10,11]. As results, in PnCs, coherence of thermal
55 phonons, whose wavelengths are only a few nanometers at room temperature, is lost

56 when scattered by nanoscale roughness and disorders. Therefore, room temperature
57 coherent transport only occurs for long-wave-length or low frequency phonons (<200
58 GHz [3,8]) with large relaxation time, but their small density of states makes the
59 contribution to thermal conductivity negligible. The logic of the above explanation is
60 true for bulk crystals but fails in the case of usual PnCs that take forms of films because
61 these low frequency coherent phonons have extremely large density of states owing to
62 the low dimensional nature of the PnCs [12,13], which will lead to the result that even
63 very low frequency coherent phonons could significantly contribute to thermal
64 conductivity when only considering three-phonon scattering mechanism for evaluating
65 intrinsic phonon relaxation time (here, intrinsic relaxation time is referred as the
66 lifetime due to phonon-phonon interaction [14]), as will be discussed later. That is to
67 say thermal conductivity of PnC cannot be explained by a boundary scattering of
68 incoherent phonons if only considering three phonon scattering. Therefore, the reason
69 for the negligible contribution of coherent phonons remain unclear.

70 In fact, the large contribution of low frequency coherent phonons suggests that more
71 detailed discussion should be given to their relaxation time. Indeed, for low frequency
72 phonons at room temperature, the consideration of only three-phonon scattering
73 mechanism is not sufficient. Experimental measurements and theoretical works have
74 shown that relaxation time of low frequency phonons (sound waves) is dominated by
75 Akhiezer damping rather than three-phonon scattering mechanism (Landau-Rumer
76 theory) in a variety of bulk materials [14-19]. The mechanism of Akhiezer damping is
77 a coupling of strain of sound waves and thermal phonons: sound wave strain disturb the
78 local occupation of thermal phonons whose frequencies depend on strain, and the
79 thermal phonons then collide with one another, returning the system to local thermal
80 equilibrium as energy is removed from the sound waves [15]. Such mechanism should
81 also affect relaxation process of coherent phonons in PnCs, which have frequencies
82 within sub-terahertz range, and are basically sound waves. Since the original work of
83 Akhiezer, the mechanism of Akhiezer was found to be important for the absorption of
84 sound waves, as well as for energy dissipation in mechanical nanoresonators [20,21],

85 however, few studies have noticed its importance in the field of heat conduction.

86 In this work, we show that Akhiezer mechanism plays an important role in heat
87 conduction for low dimensional materials like PnCs. We theoretically illustrate that
88 Akhiezer mechanism significantly reduces contribution of coherent phonons to thermal
89 conductivity of PnCs at the temperature regime from 130 K-300 K to the extent that it
90 becomes intrinsically small even when there is no roughness, thus, properly answered
91 the question that why the thermal conductivity of PnC can be explained by only
92 considering scattering of incoherent phonons.

93 **II. THEORY FOR THERMAL CONDUCTIVITY OF COHERENT** 94 **AND INCOHERENT PHONONS**

95 The total thermal conductivity κ_{Total} of thin film and PnCs includes contributions of
96 both coherent (κ_{coh}) and incoherent phonons (κ_{inc}), which is expressed as [22]:

$$97 \quad \kappa_{Total}(\omega_s) = \kappa_{coh}(\omega_s) + \kappa_{inc}(\omega_s) \quad (1)$$

98 where ω_s is the upper frequency bound of the coherent regime, in other words, the
99 switching frequency between the coherent and incoherent regimes.

100 We calculate the contribution from incoherent phonons (κ_{inc}) of thin film and PnCs
101 based on the kinetic theory, which is expressed as:

$$102 \quad \kappa_{inc}(\omega_s) = \int_{\omega_s}^{\infty} C(\omega) D_{bulk}(\omega) v_{bulk}(\omega) l(\omega) d\omega \quad (2)$$

103 where ω is the frequency; $C(\omega)$, $D_{bulk}(\omega)$, $v_{bulk}(\omega)$ denote the frequency dependent heat
104 capacity, bulk density of states and group velocity, respectively. $l(\omega)$ is the effective
105 mean free path of incoherent phonons obtained by Monte Carlo ray tracing method [23].

106 Similarly, contribution of coherent phonons to thermal conductivity (κ_{coh}) of thin film
107 and PnCs is calculated by:

108 $\kappa_{coh}(\omega_s) = \int_0^{\omega_s} C(\omega)D(\omega)v_g(\omega)^2\tau(\omega)d\omega$ (3)

109 where $D(\omega)$, $v_g(\omega)=\partial\omega/\partial q$ and $\tau(\omega)$ denote the frequency dependent density of states,
 110 group velocity, and relaxation time for coherent phonons in thin film and PnC,
 111 respectively.

112 The parameters $C(\omega)$, $D(\omega)$ and $v_g(\omega)$ in Eq. (3) can be calculated from phonon
 113 dispersions of thin film and PnCs, which is obtained by solving the continuum-based
 114 elastic wave equation using finite element method (FEM) [13]:

115 $\mu\nabla^2u + (\mu + \lambda)\nabla(\nabla \cdot u) = -\rho\omega^2u$ (4)

116 where u is the displacement vector, $\rho = 2329 \text{ kg m}^{-3}$ is the mass density of silicon crystal,
 117 $\lambda = 69.3$ and $\mu = 81.3 \text{ GPa}$ are the Láme parameters of silicon crystal.

118 As discussed in Section I, relaxation of coherent phonons is expected to take two
 119 forms: three-phonon scattering mechanism (Landau-Rumer theory) and Akhiezer
 120 damping. Relaxation time due to three-phonon scattering mechanism is approximated
 121 by Klemens model, which is widely used and validated [24,25]:

122 $\tau_K^{-1} = BT\omega^2$ (5)

123 where T is the temperature, and B is a constant often quantified empirically.

124 It should be noted that Landau-Rumer theory is also based on the concept of three-
 125 phonon scattering, however, it only includes sound-phonon-phonon interactions. Here,
 126 we use three-phonon scattering model instead as it also includes sound-sound-sound
 127 and sound-sound-phonon interactions, which is a more accurate description. On the
 128 other hand, the relaxation time of Akhiezer damping is modeled using the expression
 129 derived by Maris [17]:

130 $\tau_A^{-1} = \frac{C_v T}{\rho v^2} \cdot \frac{\omega^2 \tau_{ph} ((\gamma^2) - (\gamma)^2)}{1 + \omega^2 \tau_{ph}^2}$ (6)

131 where C_v is the specific heat capacity per volume, γ is Gununeizen parameter, v is

132 phonon phase velocity, and τ_{ph} is the averaged relaxation time of thermal phonons.

133 Here, we include the mechanisms of both three-phonon scattering and Akhiezer
134 damping into phonon relaxation time τ by using Matthiessen's rule as [14,16]:

$$135 \quad \tau^{-1} = \tau_K^{-1} + \tau_A^{-1} \quad (7)$$

136 Equation (6) shows that phonon relaxation time first yields a quadratic frequency
137 dependence for the lower frequencies, with a factor almost three orders of magnitude
138 smaller than the three-phonon scattering, and in the high-frequency limit of the
139 Akhiezer model (around tens of GHz), the lifetime is independent of frequency, and
140 becomes constant [14]. This and Eq. (7) indicate that the relaxation time of phonons
141 first follows Akhiezer model and then transits to three-phonon scattering when phonon
142 frequency becomes higher. The transition frequency between three-phonon scattering
143 and Akhiezer's damping is expected to happen around several hundred GHz, which was
144 first experimentally observed by Hasson and Many [19]. The transition zone of the two
145 scenarios was observed by Maznev *et al.* at room temperature [14].

146 **III. CONHERENT HEAT CONDUCTION**

147 **A. Structures, Dispersion Relation and Group velocity**

148 We considered a 2D silicon thin film with periodic cylindrical holes, which is the
149 most frequently studied representative PnC [3] (Fig. 1(a)). The height t , width w , and
150 hole diameter d of the PnC are set to 150 nm, 100 nm, and 80 nm, respectively. A folded
151 dispersion relation in the frequency range of 0-160 GHz (Fig. 1(b)) is obtained by
152 solving Eq. (4) with 2D periodic boundary conditions. It is shown that the folded
153 dispersion curves become flatter as frequency increases, which indicates reduction in
154 group velocity (Fig. 1(c)). Further, although the frequency-dependent profile of group
155 velocity is scattered, when smoothed by averaging the group velocities for each
156 frequency, the profile in the range between 80 and 160 GHz shows a clear power law
157 frequency dependence. An exponent of -1.41 is obtained by fitting a power law to the

158 data in this frequency range. The fitting curve was then extrapolated to obtain average
159 group velocity in higher frequency regimes. Note that the extrapolation is needed
160 because the computational load to calculate full dispersion relations of higher frequency
161 phonons would become too large. The validity of the extrapolation was confirmed by
162 calculating tens of branches of dispersion around given frequencies within 1THz, and
163 the average group velocities around given frequencies were confirmed to agree with the
164 fitting curve. With the same approach as for PnC, we also obtained group velocity of
165 thin film with the same thickness (150 nm), and only average group velocity is plotted
166 (Fig. 1(c)). It is shown that the average group velocity of thin film is larger than that of
167 the PnC because periodic structures in PnC cause larger bandgaps, which reduces group
168 velocity.

169 **B. Temperature Dependent Phonon Relaxation Time**

170 Firstly, to show the validity of the calculation, we obtained phonon relaxation time
171 of bulk silicon crystals from first principles-based lattice dynamic calculation, which
172 agrees with experimental data at a temperature range of 130 K-300 K (Fig. 2(a)). The
173 maximum difference between our calculation and experimental data is 25%. It is clear
174 that, for a given temperature, phonon relaxation time deviates from the three-phonon
175 scattering scenario, and transit to the Akhiezer damping scenario when phonon
176 frequency becomes GHz. As a result, relaxation time of low frequency phonons is
177 reduced by 3 orders. It should be noted that the transition between the two scenarios
178 has been investigated only at room temperature for Si and GaAs-AlAs superlattice [14].
179 Here, in Fig. 2(a), by comparing experiment data with our calculation, we observed that
180 the transition is take place at ~ 200 GHz for 200 K-300 K, and ~ 100 GHz for 130 K.

181 Now that the calculation is validated, we obtained relaxation time of acoustic
182 branches (< 12 GHz) for PnCs, as plotted in Fig. 2 (b), taking the case of 300 K as an
183 example. It is shown that the trend of the relaxation time for the longitudinal mode of
184 PnCs agrees with that of bulk crystals, however, the magnitude is smaller due to the
185 folding effect, which yields phonon bandgaps and reduces phase velocity v . Other

186 acoustic branches show similar characteristics. For optical phonons, instead of
187 replacing phase velocity v in Eq. (6) by group velocity v_g , as in the work of E. Chavez-
188 Angel *et al.* [26], we approximated v by the average phase velocity of all acoustic
189 branches considering that optical branches are folded acoustic ones. One can observe
190 that phonon relaxation time transits to that of three-phonon scattering as frequency
191 increases, which indicates that three-phonon scattering mechanism dominant phonon
192 decay process for high frequency phonons. Similar relaxation time transition also
193 happens for the 2D thin film, the difference is that average relaxation time of thin film
194 is larger than that of PnC due to a larger phase velocity v , which resulted from smaller
195 bandgaps in dispersions relations of thin film.

196 **C. Influence of Akhiezer Damping on Thermal Conductivity of Coherent** 197 **Phonons**

198 Next, we discuss how much the transition from three-phonon scattering to Akhiezer
199 damping can affect thermal conductivity of both bulk crystals, thin films and PnCs. We
200 first verified that such transition has negligible effect on the total thermal conductivity
201 of bulk crystals when temperature is below 300 K. As for thin films and PnCs, here we
202 assume the switching frequency ω_s as 0.2 THz, i.e. the coherent regime is 0-0.2 THz,
203 and leave the discussion of frequency dependence on the coherent regime for later, as
204 it does not affect the discussions here. It should be noted that the coherent regime is not
205 taken randomly, but matches with the case that the thin film and PnC have a 2-nm
206 surface roughness [3,8], which is the average value of the most frequently measured
207 roughness in experiment (1 nm-3 nm). The method for determining the coherent regime
208 by roughness is discussed in the Appendix. **The κ_{inc} is obtained by Monte Carlo**
209 **raytracing calculation, in which boundary scattering of incoherent phonons is included.**
210 **In case of coherent phonons behaving as waves, the boundary effect is included as the**
211 **folded dispersion of coherent phonons (Fig. 1), which are formed when the phonons**
212 **are reflected without dephasing at the periodic boundaries.**

213 A comparison of thermal conductivity of thin film and PnC with two different

214 relaxation time τ models (with and without Akhiezer) for 130 K and 300 K is shown in
 215 Fig. 3. Firstly, we discuss the results when there is only three phonon scattering. In this
 216 case, κ_{coh} of thin film within 0-0.2 THz is $5 \text{ Wm}^{-1}\text{K}^{-1}$ at 300 K and $17.8 \text{ Wm}^{-1}\text{K}^{-1}$ at 130
 217 K, which contributes about 7.4% and 15.2% of κ_{Total} for 300 K and 130 K, respectively
 218 (Fig. 3(a)). The proportion of κ_{coh} in κ_{Total} becomes even larger for PnCs due to larger
 219 density of states, which will be shown in the later discussion. At 300 K, κ_{coh} of PnC is
 220 $9.5 \text{ Wm}^{-1}\text{K}^{-1}$, which contributes 53% of κ_{Total} for PnC. At lower temperature of 130 K,
 221 κ_{coh} of PnC reaches $33.3 \text{ Wm}^{-1}\text{K}^{-1}$, and contributes to 81.1% of κ_{Total} for PnC. If this is
 222 the case, the total thermal conductivity of PnCs cannot be explained by scattering of
 223 incoherent phonons, which is not the actual situation of previous theoretical and
 224 experimental results [3-5]. As discussed in Section I and III(B), for low frequency
 225 phonons, only considering three phonon scattering is not enough, Akhiezer damping
 226 should be considered as a key issue for relaxation process of these phonons, and it can
 227 be included in phonon relaxation time using Eq. (5) and Eq. (6). For the case that Akhiezer
 228 is considered, κ_{coh} of both thin film and PnC is smaller than $0.5 \text{ Wm}^{-1}\text{K}^{-1}$ for 300 K and
 229 130 K, and the proportion of κ_{coh} in κ_{Total} is less than 1%, which indicates that κ_{coh} is
 230 negligible in both thin film and PnC for 130 K-300 K (Fig. 3(b)), and that κ_{Total} is almost
 231 dominant by the incoherent part κ_{inc} . The implication here is that, for low dimensional
 232 materials like thin film and PnCs, it is important to take Akhiezer damping into account
 233 to accurately evaluate relaxation time of low frequency phonons, otherwise, their
 234 contributions to thermal conductivity can be hugely overestimated by only considering
 235 three-phonon scattering.

236

D. Phonon Density of States

237 From Section III (C), we see that Akhiezer damping does not influence total thermal
 238 conductivity of bulk silicon crystal but has large influence on thermal conductivity of
 239 PnCs. The reason lies in density of states, $D(\omega)$ (Fig. 4). In bulk crystal, $D(\omega)$ is
 240 proportional to ω^2 , which indicates that $D(\omega)$ of low frequency phonons is very small.
 241 Therefore, even relaxation time of these phonons is overestimated by only considering
 242 the ω^{-2} -dependent three-phonon scattering, their contributions to the total thermal

243 conductivity of bulk silicon crystal is still negligible, in other words, we do not need to
244 consider Akhiezer damping effect on the thermal conductivity of bulk crystal below
245 300 K.

246 However, in PnCs, $D(\omega)$ transits from 3D, 2D to 1D as frequency decreases due to
247 coherent effect, and accordingly, the frequency dependence of $D(\omega)$ changes from ω^{-2} ,
248 ω^{-1} to ω^0 . As a result, $D(\omega)$ of low frequency phonons in thin film and PnC is much
249 larger than $D(\omega)$ in bulk crystals, which leads to a significant overestimation of κ_{coh} in
250 thin film and PnCs when only considering the ω^{-2} -dependent three-phonon scattering
251 for intrinsic relaxation time. We also noticed that, in the case that without Akhiezer
252 damping, κ_{coh} for PnC is larger than κ_{coh} of thin film (Fig. 3(a)), even phonon group
253 velocity is larger for thin film (Fig. 1). This is because $D(\omega)$ of acoustic phonon (< 12
254 GHz) in PnCs is four times larger than $D(\omega)$ of acoustic phonon in thin film, which
255 would lead to severer overestimation κ_{coh} for PnC.

256 The conclusion for Section III is that, although the existence of a 2-nm surface
257 roughness makes the coherent regimes very small (0-0.2 THz), density of states of the
258 low frequency coherent phonons is much larger than that of bulk silicon crystals,
259 therefore, these phonons have large potential to contribute to thermal conductivity when
260 only three phonon scattering is considered. However, when Akhiezer mechanism is
261 involved, relaxation time of these phonons is hugely reduced, as a result, the proportion
262 of κ_{coh} in κ_{Total} for both thin film and PnC is negligible ($< 1\%$), that is why the total
263 thermal conductivity of thin film and PnC, κ_{Total} can be explained by only considering
264 the contributions of incoherent phonons κ_{inc} .

265 Current result is consistent with the recent experimental and theoretical works on
266 thin film PnCs [3][4][5]. They have successfully reproduced the experimental results
267 with Monte Carlo calculations by ignoring the contribution of sub-THz phonon to
268 thermal conductivity. The fact the calculation could reproduce the experiments means
269 that the Akhiezer damping has suppressed the phonon relaxation time, and that the
270 works are consistent with our work. Although the actual geometry of our PnC and these

271 works are different, the above discussion on the dimension and contribution of sub-THz
272 phonon contribution should be applicable to PnC with thickness and holes on the order
273 of 100 nm.

274 **IV. SWITCHING-FREQUENCY DEPENDENT COHERENT** 275 **AND INCOHERENT HEAT CONDUCTION**

276 So far, our discussion has been based on the assumption that the roughness of the
277 thin film and PnC is 2 nm, and the switching frequency ω_s is ω_0 (=0.2 THz). **However,**
278 **the ω_s can change when roughness on the surface is modified. Therefore, in what**
279 **follows, we consider ω_s as a variable to investigate contributions of coherent phonons**
280 **to thermal conductivity. Note that this also helps gain understanding of the case with**
281 **no roughness, which is the theoretical upper limit of contribution of coherent phonons.**
282 Nevertheless, we can determine the maximum value of ω_s using the criterion that MPF
283 of bulk phonons should be at least larger than several periods of periodic structures in
284 PnCs (here, it is 100 nm). The reason is that coherent length should be smaller than
285 MFP bulk phonons, and MFP are required to be sufficient long such that they can cross
286 several periodicities, thereby creating many secondary waves to achieve interference
287 effect, which results in the folded dispersion relation of PnCs [6]. The minimum number
288 of periodicity is two (that is phonon passes though the PnC and then be reflected back),
289 which gives the upper bound of ω_s .

290 If $\omega_s < \omega_0$, κ_{coh} within $0-\omega_s$ can be directly calculated by Eq. (3) with their full
291 dispersion relations, whereas if $\omega_s > \omega_0$, contributions of coherent phonons from ω_0 to
292 ω_s is estimated by the averaging method due to a lack of information in full dispersion
293 relation. In the averaging method, we approximate the phonon group velocity and
294 density of states in Eq. (1) with the averaged group velocity obtained by the fitting
295 curve (Fig. 1(c)), and bulk phonon density of states (Fig. 4), respectively. The latter
296 approximation is based on the observation that density of states of PnCs and bulk crystal
297 are roughly the same for frequencies above ω_0 (Fig. 4). Then, the switching-frequency

298 dependent $\kappa_{\text{coh}}(\omega_s)$ of PnC or thinfilm can be expressed as:

$$299 \quad \kappa_{\text{coh}}(\omega_s) = \kappa_0 + \int_{\omega_0}^{\omega_s} C(\omega) D_{\text{bulk}}(\omega) v_{\text{av}}(\omega)^2 \tau(\omega) d\omega \quad (8)$$

300 where κ_0 is the contribution of coherent phonons with frequencies between 0 and ω_0 ,
301 and the second term represents contribution of coherent phonons with frequencies
302 between ω_0 and ω_s , where $v_{\text{av}}(\omega)$ is the averaged group velocity and $D_{\text{bulk}}(\omega)$ is the bulk
303 phonon density of states.

304 For thin film and PnC at 300 K (Fig. 5(a) and Fig. 5(c)), the maximum coherent
305 regime is determined as 0-3.0 THz. We found that κ_{coh} of both thin film and PnC are
306 negligible when compared to κ_{inc} even ω_s reaches its maximum (3 THz). The results
307 indicate that κ_{coh} contributes a very small proportion of κ_{Total} for both thin film and at
308 300 K, even there is no roughness effect. This is because of two reasons: one is that
309 Akhiezer damping significantly reduces relaxation time of phonons in the Akhiezer
310 regime (<0.2 THz for 300 K, Fig. 3(b)), and the other is that the group velocity of
311 phonons in three-phonon-scattering regime (0.2 THz-3.0 THz, Fig. 3(b)) is small due
312 to phonon bandgaps that are caused by the folding effect. As a result, contributions of
313 phonons within the whole coherent regime are limited.

314 As temperature decreases to 130 K (Fig. 5(b) and Fig. 5(d)), the maximum value of
315 ω_s increased to 4 THz, and Akhiezer damping is weakened due to a reduction in thermal
316 phonons population. Therefore, relaxation time of coherent phonons increases (Fig. 2),
317 however, Akhiezer damping still has strong influence on κ_{coh} of thin film and PnC. For
318 the PnC at 130 K, the maximum value of κ_{coh} is only $0.1 \text{ Wm}^{-1}\text{K}^{-1}$. In thin film, the
319 value of κ_{coh} is larger when comparing with κ_{coh} for PnC, and can contribute to $5.8 \text{ Wm}^{-1}\text{K}^{-1}$
320 when ω_s reaches to its maximum (4 THz). This is because group velocity of three-
321 phonon scattering regime (0.1 THz -4 THz for 130 K) is larger than that of PnC (Fig.
322 1). However, the proportion of κ_{coh} in κ_{Total} is still small ($<8\%$). We also noticed that for
323 both thin film and PnC, sub-THz phonons contributes to the most part of κ_{coh} , and
324 above-THz coherent phonons does not contribute much to κ_{coh} due to their small group

325 velocity and relaxation time (Fig. 1(c) and Fig. 2).

326 Taking the most extremely case (no roughness) as an example, a comparison of
327 thermal conductivity of thin film and PnC with two different relaxation time τ models
328 at 130 K and 300 K is shown in Fig. 6. The discussion here is similar with Section
329 III(C). The coherent part, κ_{coh} can contribute a large part of κ_{Total} when without
330 considering Akhiezer damping. In thin film, κ_{coh} can contribute about 11.2% and 28%
331 of κ_{Total} for 300 K and 130 K, respectively. For PnC, contributions of κ_{coh} can even reach
332 to 56% at 300 K and 85% of κ_{Total} . However, Akhiezer damping can reduced the
333 proportion to less than 2% for PnC at both 300 K and 130 K, and for thin film, the
334 proportion is less than 2% at 300 K and around 8% at 130 K. The value of the
335 proportions here is a litter larger than that in Section III(C), however, it is still small.
336 Therefore, we can conclude that the coherent phonons contribution κ_{coh} to the total
337 thermal conductivity κ_{Total} for both thin film and PnC is very small even there is no
338 roughness, or the κ_{Total} for both thin film and PnC can be explained by the contributions
339 of incoherent phonons.

340 Finally, it should be noted that currently our calculation here cannot deal with the
341 cases for temperatures that below 130 K. The reason is that Ahkiezer mechanism, as
342 original developed, only valid at high temperatures, however, up to date, the exact valid
343 temperature regime is not known. We can extend our calculation to 130 K because the
344 experimental measurements match with theoretical calculations (Fig. 2). More
345 experimental measurements are still need below 130 K. On the other hand, the equation
346 for Ahkiezer damping (Eq. (6)) includes average phonon relation time of bulk silicon
347 crystal (τ_{ph}), which is often obtained by single phonon relaxation time approximation.
348 However, the single phonon relaxation time approximation for the Boltzmann equation
349 may not valid at lower temperatures. We hope that lower temperature measurements
350 and deeper theoretical analysis for phonon relaxation time in both bulk and
351 nanostructured materials will become available soon.

352

V. CONCLUSIONS

353

354 In conclusion, we show that average group velocity of high frequency coherent
355 phonons in thin film and PnC can be approximated by the exponential function $\omega^{-\beta}$
356 ($\beta=0.66$ and 1.41 for our thin film and PnC samples, respectively), which indicates that
357 high frequency phonons has smaller group velocities, and thus contribute less to thermal
358 conductivity. Then, we show that low frequency coherent phonons in low dimension
359 materials like PnCs have extremely large density of states due to the low dimension
360 nature, which could significantly contribute to thermal conductivity when only
361 considering three phonon scattering. However, by comparing experiment data with our
362 calculation, we show that Akhiezer damping is dominant and should be considered
363 when dealing with relation time of low frequency phonons (<200 GHz for 200 K-300
364 K, and <100 GHz for 130 K). Because of Akhiezer damping, coherent phonons
365 contribution is reduced to the extent that their contribution to total thermal conductivity
366 of thin film and PnC at 130 K-300 K becomes very small ($<8\%$), even there is no surface
367 roughness, that is why the total thermal conductivity of thin film and PnC can be
368 explained by only considering the incoherent phonons contributions.

369

370 APPENDIX

371 In this section, we evaluate switching frequency ω_s as a function of roughness
372 according to the work of M. R. Wagner *et al* [8]:

$$373 \quad \omega_s = \frac{2\pi V_s}{R} \sqrt{\frac{-\ln(P)}{16\pi^3}} \quad (9)$$

374 where R is the roughness size (including surface roughness, hole wall roughness, lattice
375 site displacement, disorder etc.); P is the specularity, here we use $P=0.3$ to define the
376 boundary of coherent and incoherent regimes, i.e. the ω_s ; V_s is the longitudinal sound
377 velocity as 8433 m/s [8].

378 Switching frequency as a function of roughness size R is shown in Fig. 7, from which
379 we can obtain 0.2 THz for ω_s when $R=2$ nm. In the works of M. R. Wagner *et al*, $P=0.5$,
380 here we use 0.3 just for a more conservative estimation.

381

382 ACKNOWLEDGMENTS

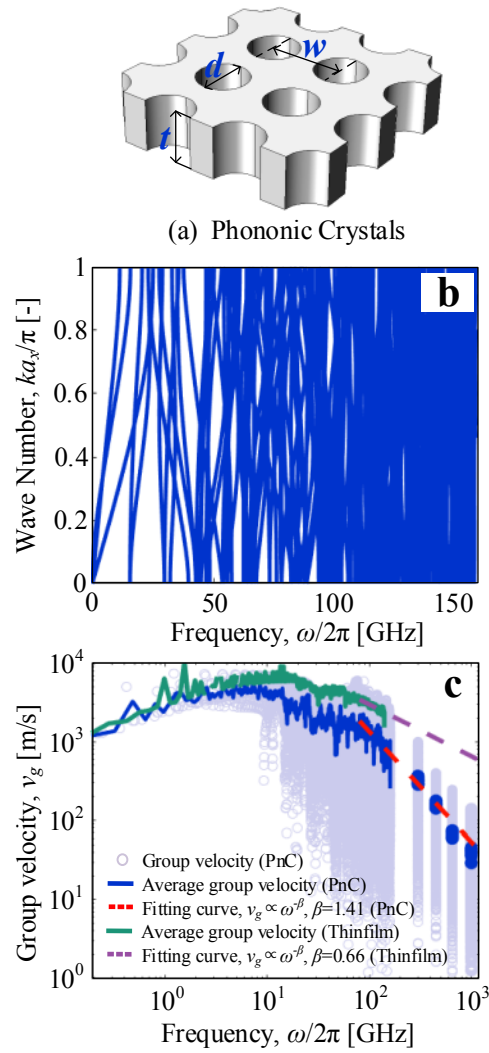
383 This work was partially supported by CREST “Scientific Innovation for Energy
384 Harvesting Technology” (Grant No. JPMJCR16Q5) and Grant-in-Aid for Scientific
385 Research (B) (Grant No. JP16H04274) from JSPS KAKENHI and JSPS KAKENHI
386 Grant No. JP18J14024, Japan, and the China Scholarship Council.

387

388 References

- 389 [1] J. K. Yu, S. Mitrovic, D. Tham, J. Varghese, and J. R. Heath, *Nature Nanotechnology* **5**,
390 718 (2010).
- 391 [2] N. Zen, T. A. Puurtinen, T. J. Isotalo, S. Chaudhuri, and I. J. Maasilta, *Nature*
392 *Communications* **5**, 3435 (2014).
- 393 [3] J. Maire, R. Anufriev, R. Yanagisawa, A. Ramiere, S. Volz, and M. Nomura, *Science*
394 *Advances* **3**, e1700027 (2017).
- 395 [4] J. Lee, W. Lee, G. Wehmeyer, S. Dhuey, D. L. Olynick, S. Cabrini, C. Dames, J. J. Urban,
396 and P. D. Yang, *Nature Communications* **8**, 14054 (2017).
- 397 [5] K. D. Parrish, J. R. Abel, A. Jain, J. A. Malen, and A. J. H. McGaughey, *Journal of Applied*
398 *Physics* **122**, 125101 (2017).
- 399 [6] M. Maldovan, *Nature Materials* **14**, 667 (2015).
- 400 [7] N. K. Ravichandran and A. J. Minnich, *Physical Review B* **89**, 205432 (2014).
- 401 [8] M. R. Wagner, B. Graczykowski, J. S. Reparaz, A. El Sachat, M. Sledzinska, F. Alzina,
402 and C. M. S. Torres, *Nano Letters* **16**, 5661 (2016).
- 403 [9] T. Oyake, L. Feng, T. Shiga, M. Isogawa, Y. Nakamura, and J. Shiomi, *Physical Review*
404 *Letters* **120**, 045901 (2018).
- 405 [10] M. N. Luckyanova *et al.*, *Science* **338**, 936 (2012).
- 406 [11] J. Ravichandran *et al.*, *Nature Materials* **13**, 168 (2014).
- 407 [12] F. Kargar, B. Debnath, J. P. Kakko, A. Saynatjoki, H. Lipsanen, D. L. Nika, R. K. Lake,
408 and A. A. Balandin, *Nature Communications* **7**, 13400 (2016).
- 409 [13] R. Anufriev and M. Nomura, *Physical Review B* **91**, 245417 (2015).
- 410 [14] A. A. Maznev, F. Hofmann, A. Jandl, K. Esfarjani, M. T. Bulsara, E. A. Fitzgerald, G.
411 Chen, and K. A. Nelson, *Applied Physics Letters* **102**, 041901 (2013).
- 412 [15] B. C. Daly, K. Kang, Y. Wang, and D. G. Cahill, *Physical Review B* **80**, 174112 (2009).
- 413 [16] A. A. Maznev, J. A. Johnson, and K. A. Nelson, *Physical Review B* **84**, 195206 (2011).
- 414 [17] H. J. Maris, *Physical Review* **175**, 1077 (1968).
- 415 [18] T. O. Woodruff and H. Ehrenreich, *Physical Review* **123**, 1553 (1961).
- 416 [19] J. Hasson and A. Many, *Physical Review Letters* **35**, 792 (1975).
- 417 [20] K. Kunal and N. R. Aluru, *Physical Review B* **84**, 245450 (2011).

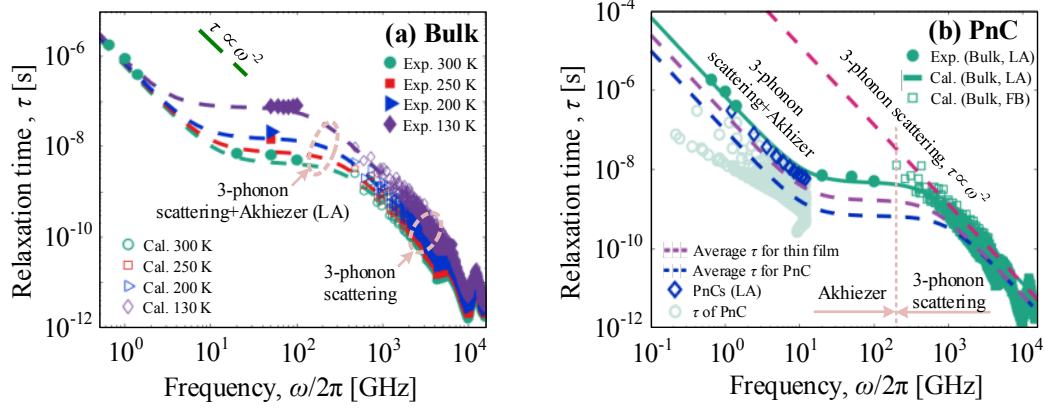
418 [21] J. Atalaya, T. W. Kenny, M. L. Roukes, and M. I. Dykman, *Physical Review B* **94**, 195440
419 (2016).
420 [22] S. Alaie, D. F. Goettler, M. Su, Z. C. Leseman, C. M. Reinke, and I. El-Kady, *Nature*
421 *Communications* **6**, 7228 (2015).
422 [23] T. Hori, J. Shiomi, and C. Dames, *Applied Physics Letters* **106**, 171901 (2015).
423 [24] B. L. Davis and M. I. Hussein, *Physical Review Letters* **112**, 055505 (2014).
424 [25] H. Honarvar and M. I. Hussein, *Physical Review B* **93**, 081412 (2016).
425 [26] E. Chavez-Angel, R. A. Zarate, J. Gomis-Bresco, F. Alzina, and C. M. S. Torres,
426 *Semiconductor Science and Technology* **29**, 124010 (2014).
427 [27] J. Y. Duquesne and B. Perrin, *Physical Review B* **68**, 134205 (2003).
428 [28] H. Y. Hao and H. J. Maris, *Physical Review B* **63**, 224301 (2001).
429 [29] M. Pomerantz, *Physical Review* **139**, A501 (1965).
430
431
432



434

435 **Fig. 1** (a) Schematic of two-dimensional silicon phononic crystal (PnC). $t=150$ nm,
 436 $w=100$ nm and $d=80$ nm denotes the height, width, and hole diameter of the PnC,
 437 respectively. (b) phonon dispersion relation of PnC along G-X. (c) frequency-dependent
 438 group velocity of PnCs and thin film phonons.

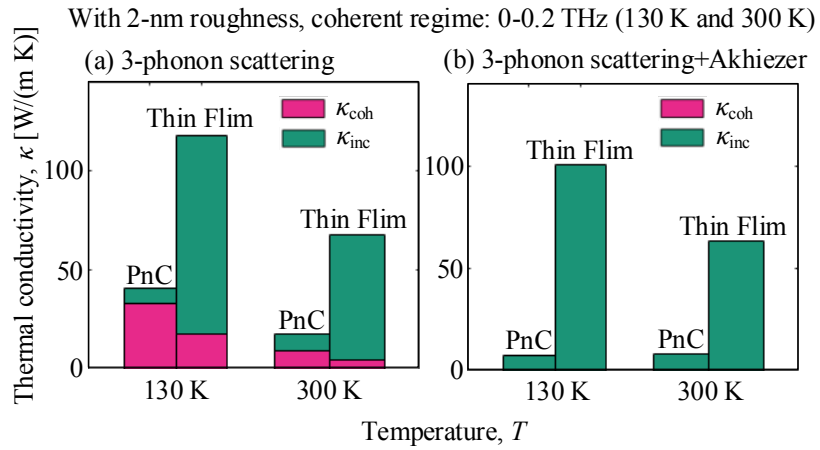
439



440

441 **Fig. 2** (a) Frequency and temperature dependent phonon relaxation time for bulk silicon
 442 crystals. The dashed lines are calculated results for longitudinal modes (LA) at different
 443 temperatures. Experimental data are measured results for LA modes and are taken from
 444 the references [15,27-29] (b) Frequency-dependent relaxation time of thin film and
 445 PnCs at 300 K, and a comparison with bulk phonon relaxation time for LA modes and
 446 modes in Full Brillion zone (FB). The boundary of Akhiezer and 3-phonon scattering
 447 regimes at 300 K is around 200 GHz. **Note that “3-phonon scattering+Akhiezer” in Fig.**
 448 **2 means the relaxation time calculated using Eq. (7)**

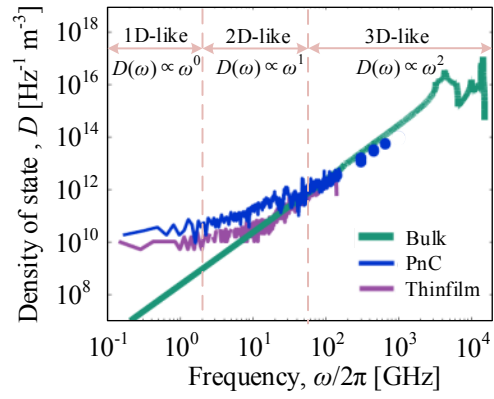
449



450

451 **Fig. 3** A comparison of thermal conductivity of thin film and PnC with two different
 452 relaxation time τ models at 130 K and 300 K for a 2-nm roughness. (a) τ model: only
 453 three-phonon scattering; (b) τ model: three-phonon scattering and Akhiezer damping.
 454 Coherent regime is determined as 0-0.2 THz for 300 K and 130 K when there is a 2-nm
 455 roughness.

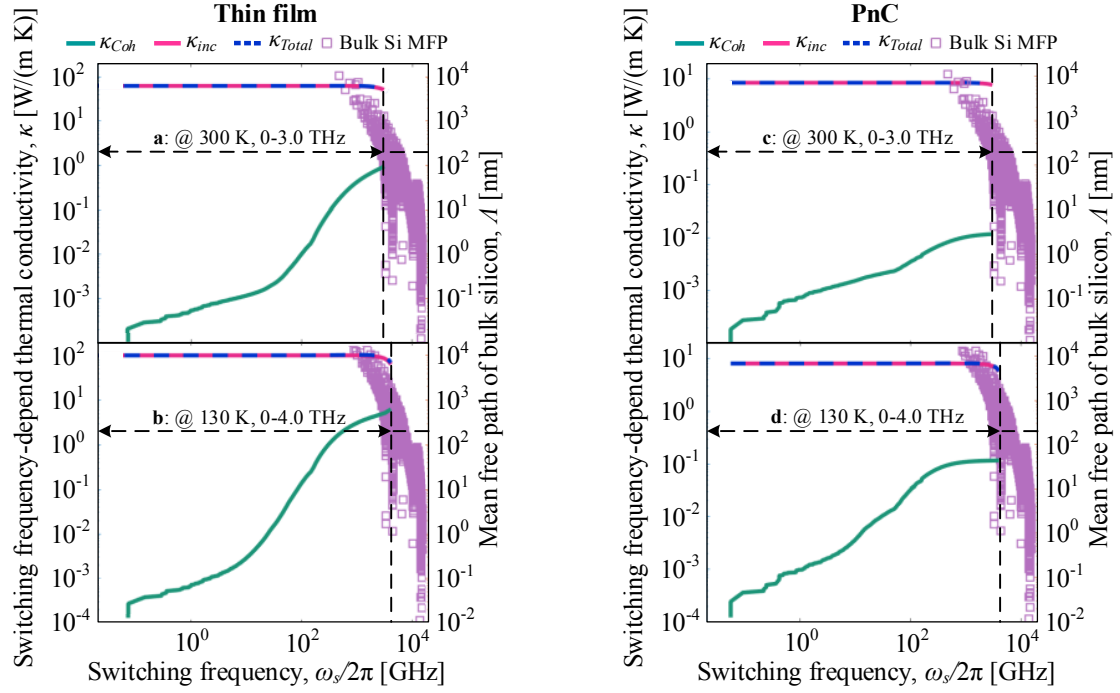
456



457

458 **Fig. 4** Frequency-dependent density of states $D(\omega)$ of thin film and PnCs, and a
 459 comparison with density of states of bulk silicon crystals

460



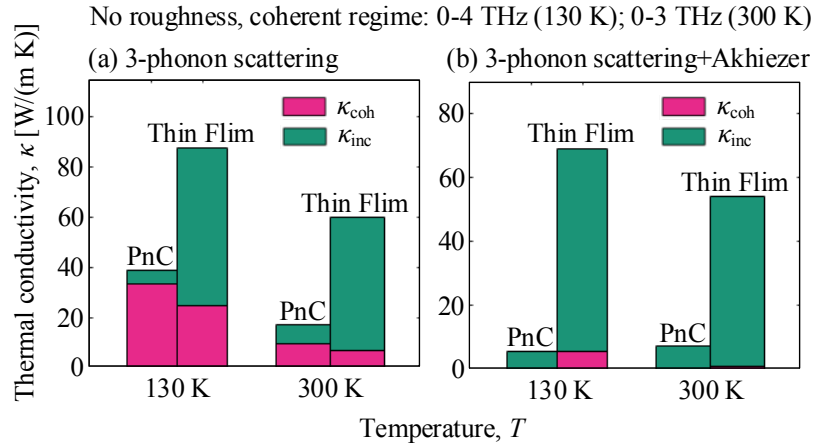
461

462 **Fig. 5** Contributions of coherent and incoherent phonons to total thermal conductivity

463 of thin film and PnCs as a function of switching frequency at 300 K and 130 K. The

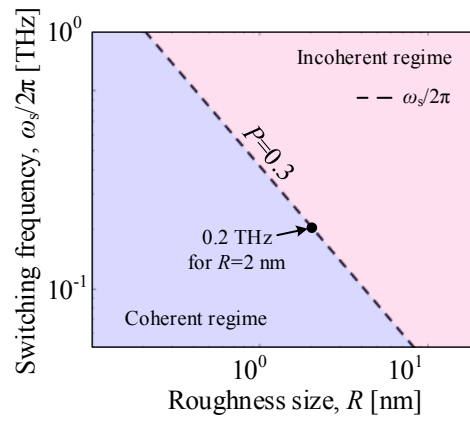
464 maximum coherent regime is determined as 0-3 THz at 300 K, and 0-4 THz at 130 K.

465



466

467 **Fig. 6** A comparison of thermal conductivity of thin film and PnC with two different
 468 relaxation time τ models at 130 K and 300 K for the most idea case (no roughness). (a)
 469 τ model: only three-phonon scattering; (b) τ model: three-phonon scattering and
 470 Akhiezer damping. Coherent regime is respectively determined as 0-3 THz and 0-4
 471 THz for 300 K and 130 K when there is no roughness.



472

473 **Fig. 7** Switching frequency as a function of roughness size R (surface roughness, hole
 474 wall roughness, lattice site displacement, hole disorder etc.) for selected specularity
 475 parameters $P=0.3$.